



**HAL**  
open science

## Batch sorption and fixed-bed elution for Pd recovery using stable amine-functionalized melamine sponge

Chuande Yu, Zhaojiang Wu, Shengye Wang, Qilong Zhong, Bo Yang, Jiajie Xu, Ke Xiao, Guibal Eric

### ► To cite this version:

Chuande Yu, Zhaojiang Wu, Shengye Wang, Qilong Zhong, Bo Yang, et al.. Batch sorption and fixed-bed elution for Pd recovery using stable amine-functionalized melamine sponge. *Journal of Cleaner Production*, 2022, 337, pp.130475. 10.1016/j.jclepro.2022.130475 . hal-03533796

**HAL Id: hal-03533796**

**<https://imt-mines-ales.hal.science/hal-03533796>**

Submitted on 23 May 2022

**HAL** is a multi-disciplinary open access archive for the deposit and dissemination of scientific research documents, whether they are published or not. The documents may come from teaching and research institutions in France or abroad, or from public or private research centers.

L'archive ouverte pluridisciplinaire **HAL**, est destinée au dépôt et à la diffusion de documents scientifiques de niveau recherche, publiés ou non, émanant des établissements d'enseignement et de recherche français ou étrangers, des laboratoires publics ou privés.

# Batch sorption and fixed-bed elution for Pd recovery using stable amine-functionalized melamine sponge

Chuande Yu<sup>a,1</sup>, Zhaojiang Wu<sup>a,1</sup>, Shengye Wang<sup>a,1</sup>, Qilong Zhong<sup>a</sup>, Bo Yang<sup>a</sup>, Jiajie Xu<sup>a</sup>, Ke Xiao<sup>a,\*</sup>, Eric Guibal<sup>b</sup>

<sup>a</sup> College of Chemistry and Environmental Engineering, Shenzhen University, Shenzhen, 518060, China

<sup>b</sup> IMT – Mines Ales, Polymers Hybrids and Composites (PCH), 6 Avenue De Clavières, F-30319, Alès Cedex, France

## A B S T R A C T

Sorption-based techniques have been widely studied for metal recovery. Conventionally, sorption and desorption steps are operated in fixed-bed column system under one-pass mode (FO); however, such sorption requires a large volume of solution passing the bed when the feed concentration is low. In this study, highly stable amine-coated alginate melamine (ML/APG) sponge was prepared and applied in a combined process involving sorption under fixed-bed recirculation mode (FR, simulating batch system) and desorption under FO for Pd(II) concentration. The efficiency was evaluated in terms of both recovery of Pd(II) and utilization of the sponge. Results show that ML/APG sponge is stable in 3 M of nitric acid, sodium hydroxide and sodium chloride after shaking at 300 rpm for 72 h with mass loss less than 0.9%. The maximum sorption capacity obtained by Langmuir model for Pd(II) increases from 9.7 mg g<sup>-1</sup> to 134.3 mg g<sup>-1</sup> after amine functionalization. The sorption equilibrium could be achieved by a less amount of solution and less time when using FR compared to FO. For example, it only needs 0.7 L of Pd(II) solution with a metal concentration of 20 mg L<sup>-1</sup> to achieve the maximum sorption capacity under FR, while the required volume is 1.8 L at flow rate of 1 mL min<sup>-1</sup> and more than 5 L at 10 mL min<sup>-1</sup> under FO. This means that FR improved the rational use of the sorbent and thus increased sorption efficiency. For elution step, FO only required 40 mL to completely desorb Pd(II) from exhausted sponge, while that needed more than 200 mL under FR. The combined process allows both effective sorption and elution. The reusability of ML/APG sponge and Pd(II) recovery from low-concentration solution were studied by combining FR for sorption step and FO for elution step. Results show that the sorption efficiency maintains more than 96% after 100 min of reaction during 10 cycles. The elution performance is stable with a 100% desorption efficiency by passing 50 mL of acidic thiourea solution. The concentration factor (CF, ratio of metal concentration in the eluate over its concentration in the sorption used for sorption), is above or close to 70 for the first 10 mL-sample and much more than 40 for the second 10 mL-sample.

### Keywords:

Fixed bed  
Recirculation  
Palladium  
Recovery  
Amine-functionalized melamine sponge

## 1. Introduction

Palladium (Pd), one of the platinum group metals, has been principally employed in autocatalysts. Waste catalysts are constantly being produced periodically because of the limitation of their lifetime. Recovery of the metal from the waste catalysts seems to be lucrative and essential for fulfilling Pd needs. The good performance of hydrometallurgical leaching followed by other recovery methods makes this technique widely employed in developing countries. However, concentration of Pd(II) in leaching liquors resulting from waste catalysts

is generally low (in the range of 5.6–50 mg L<sup>-1</sup> (Prasetyo and Anderson, 2020; Kononova et al., 1998)), making Pd recovery process from those solutions rather challenging.

Sorption has been applied not only for the removal of aqueous contaminants but also for the recovery of precious metals (Pinto et al., 2021; Garcia et al., 2021). Different modes of application of sorption techniques have been tested in the laboratory and/or at pilot scale. Fixed-bed column has many advantages such as operation at quasi-isothermal condition and no requirement of solid-liquid separation. Moreover, when packed in a fixed-bed column, the sorbents are subjected neither to high-speed shaking nor to strong agitation, making

\* Corresponding author.

E-mail address: xiaoke@szu.edu.cn (K. Xiao).

<sup>1</sup> These authors contributed equally to this work.

## Abbreviations

CF	Concentration Factor
FO	Fixed-bed system with one-pass mode
FR	Fixed-bed system with recirculation mode
ML	Melamine
PEI	Polyethyleneimine
GA	Glutaraldehyde
APG	Alginate/Polyethyleneimine-glutaraldehyde composite
SI	Supplementary Information section
LA	Loading amount
PFORE	Pseudo-first order rate equation
PSORE	Pseudo-second order rate equation
FTIR	Fourier transform infrared spectrophotometer
FESEM	Field emission scanning electron microscope
EDS	Energy-dispersive X-ray spectroscopy

the sorption system more stable. However, the conventional fixed-bed system with one-pass mode (FO) requires a larger volume of feed solution to obtain the maximum sorption capacity, while a system based on recirculation mode (FR), which is simulating batch system, can solve such a problem. On the other hand, FR is not in favor of desorption process (Yang et al., 1989). A high desorption efficiency requires a large volume of desorption agent, but this, in turn, decreases CF. A combination of these two modes, to some degree, can avoid such restrictions. The solute can be sorbed quickly from a large quantity of dilute solution under FR, and the following elution stage can be processed under FO. Therefore, the maximum desorption efficiency can be achieved using the smallest volume of desorption reagent, achieving a high CF.

Due to resistance to intraparticle mass transfer, sorbents are usually made into small particles to improve sorption kinetics. However, small particles have proved to be inappropriate for use in column systems since they may cause column clogging and serious hydrodynamic limitations. Thus, porous polymeric beads (Gao et al., 2020) and sponges (Zuhra et al., 2021) are promising materials used as sorbents. However, to maintain the porous structure, the materials either have to be stored in water (Cataldo et al., 2015) or submitted to strict drying processes (Zuhra et al., 2021; Yang et al., 2021). This brings transportation challenges or makes preparation process energy-inefficient.

(Yang et al., 1989) Melamine (ML) sponge, formaldehyde-melamine-sodium bisulfite copolymer, is a commercially available and inexpensive material. It has been widely chemically modified and applied for oil separation (Duman et al., 2021; Niu et al., 2021) or aqueous contaminant removal (Gao et al., 2021; Li et al., 2021). Although ML sponge does not have a high sorption capacity for Pd(II), it is good support for polymeric materials owing to its advantages such as high porosity and high resilience. The coating of active materials improves sorption performance for Pd(II), and the intrinsic porous structure of ML sponge, in turn, avoids strict drying processes. The composites are suitably applied in fixed-bed systems. However, to our knowledge, the amine functionalization of ML sponge for Pd(II) recovery has not been studied so far.

Here, we prepared a highly stable amine-functionalized ML sponge by a double-crosslinking process involving polyethyleneimine (PEI) grafting mediated by alginate and glutaraldehyde (GA) crosslinking processes. The sponge was tested for Pd(II) recovery. The sorption and desorption under different modes (i.e., FR and FO) have been compared. The recovery of Pd(II) from simulated leach liquors and the reusability of the sponge have also been evaluated though 10 cycles of sorption under FR and desorption under FO. The novelties of this study are: 1) preparing a highly stable amine-functionalized melamine sponge by a double-crosslinking process; 2) proposing a combined process involves FR for sorption and FO for elution to achieve a high concentration factor

for Pd(II) recovery.

## 2. Experimental

### 2.1. Materials

Melamine (ML) sponge ( $50 \times 50 \times 2$  cm, 42.5 g) was obtained from a local supermarket in Shenzhen. Alginate, branched polyethyleneimine (PEI, molecular weight =  $800 \text{ g mol}^{-1}$ ), glutaraldehyde (GA, 50% (w/w) in water), and palladium chloride (99.99%) were purchased from Macklin Biochemical Co., Ltd (Shanghai, China). The Pd(II) stock solution was prepared by dissolving 1 g Pd(II) into 1 L of 0.05 M hydrochloric acid solution (the ratio of chloride and palladium ions in stock solution is 0.05 M/1 g Pd).

### 2.2. Preparation of alginate/PEI-GA melamine (ML/APG) sponge

The preparation process of the functionalized sponge is schematically illustrated in Fig. 1a. The melamine sponge ( $20 \times 40 \times 2$  cm, 13.7 g) was firstly immersed in 300 mL alginate (1.5%). The air of the sponge was squeezed out to ensure the pores were filled with alginate. The sponge fully impregnated with alginate solution was taken out and shook with 300 mL PEI solution (5.0%, w/w) (at pH of 6.7 adjusted by  $\text{HNO}_3$ ) at 150 rpm for 24 h to ensure the complete crosslinking. The mixture was transferred to 300 mL of GA solution (5.0%) and shook for 10 h. The crosslinked alginate/PEI-GA melamine (ML/APG) sponge was then thoroughly washed and dried in air. The loading amount (LA, %) of APG on ML sponge was calculated by the following equation:  $\text{LA} = (\text{m}_2 - \text{m}_1) / \text{m}_2$ , where  $\text{m}_1$  and  $\text{m}_2$  refers to the mass of ML used for functionalization and ML/APG obtained, respectively.

### 2.3. Sorption and desorption processes

**Sorption:** The sponge was cut into cylindrical pieces (radius = 1.0 cm,  $h = 4.0$  cm for ML and  $h = 1.0$  cm for ML/APG; mass =  $106 \pm 2$  mg) and packed in a suitable holder. The solution containing Pd(II) was pumped from bottom to top through the sponge under FR or FO (shown in Fig. S1, see SI). Two milliliters of the solution were taken, filtrated through  $0.22 \mu\text{m}$  pore size membrane and analyzed by inductively coupled plasma optical emission spectrometer (ICP-OES, AVIO 200, Perkin Elmer, USA).

**Desorption:** The metal-loaded sorbents were obtained under FO. The metal-loaded sponges were washed with pure water once prior to elution step under FR or FO. The eluent solutions were diluted before being analyzed.

**Reuse:** A combination of FR for sorption step and FO for elution step was proposed for Pd(II) concentration and sponge recycling. For sorption step, 1 L of Pd(II) solution with a concentration of  $6 \text{ mg L}^{-1}$  at pH 1 was pumped through ML/APG sponge. For elution, 50 mL of acidic thiourea was used. The sponge after each desorption process was washed with 25 mL of pure water under FO before being used for next cycle.

The characterizations of ML and ML/APG sponges are given in the Supplementary Information section (SI).

### 2.4. Sorption modeling

Sorption kinetics were modeled using conventional equations such as the pseudo-first order rate equation (PFORE) and the pseudo-second order rate equation (PSORE).

The sorption processes can be controlled by a series of diffusion steps (including resistances to bulk diffusion, film diffusion and intraparticle diffusion) and by the proper reaction rate (which may obey to simple rate equations such as pseudo-first order rate equation (PFORE), Equation (1), or pseudo-second order rate equation (PSORE), Equation (2)) and the resistance to the intraparticle diffusion equation (IPD, Equation

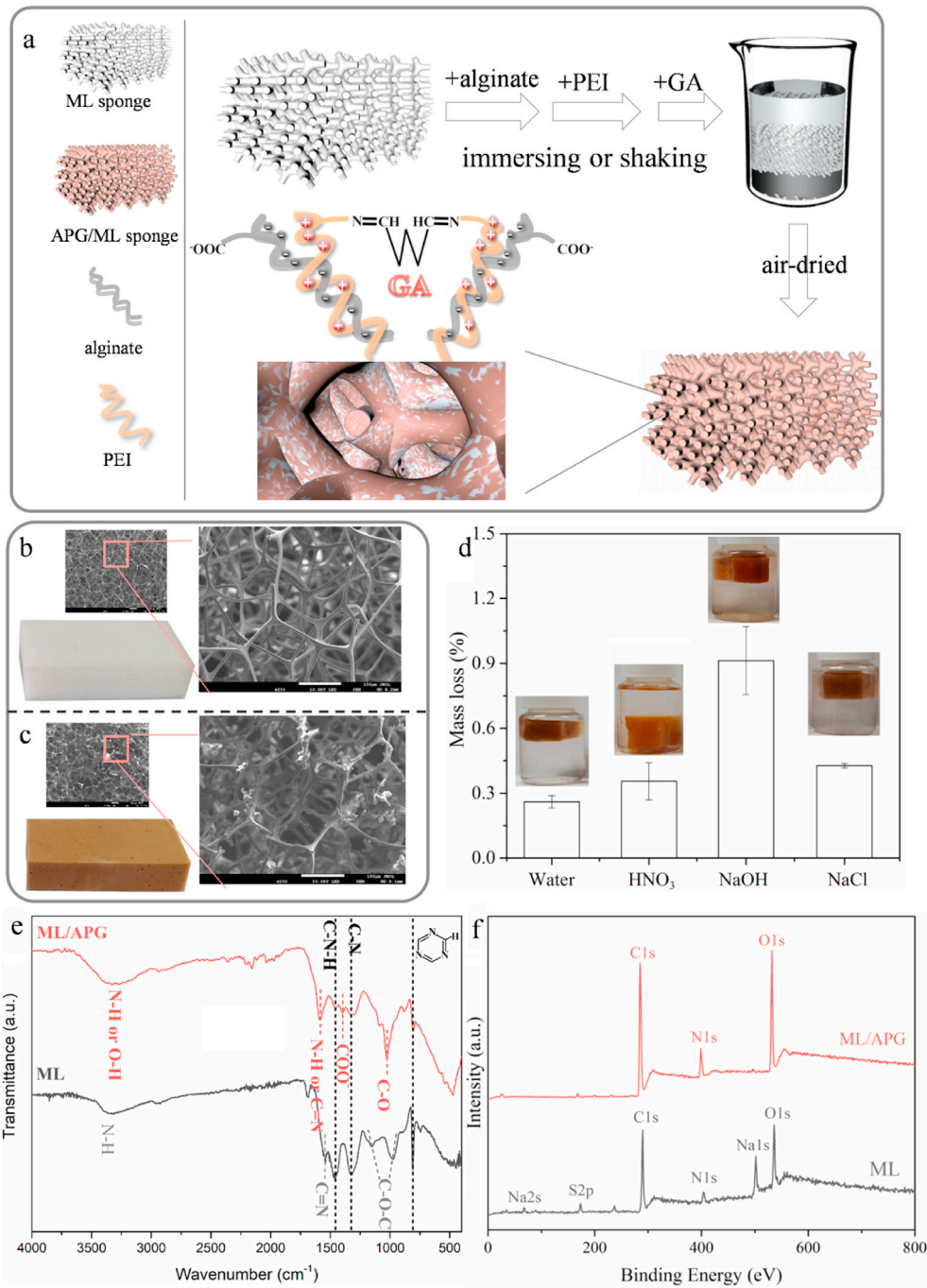


**Fig. 1.** (a) Preparation of ML/APG sponge; SEM images of (b) ML and (c) ML/APG sponges; (d) stability of ML/APG sponge shook in different solutions for 72 h; (e) XPS survey and (f) FTIR spectra for ML and ML/APG sponges. Note: the concentration of HNO<sub>3</sub>, NaOH, and NaCl used for stability test was 3 M.

(3)

$$q_t = q_{eq}(1 - e^{-k_1 t}) \quad (1)$$

$$q_t = \frac{q_{eq}^2 k_2 t}{1 + q_{eq} k_2 t} \quad (2)$$

$$q_t = k_{id} \sqrt{t} + C \quad (3)$$

where  $q_t$  and  $q_{eq}$  (mg g<sup>-1</sup>) are the sorption capacities sorbed at  $t$  (min) and at equilibrium, respectively. The parameters  $k_1$ ,  $k_2$  and  $k_{id}$  refer to the apparent rate constants of PFORE (min<sup>-1</sup>), PSORE (g mg<sup>-1</sup> min<sup>-1</sup>) and IPD (mg g<sup>-1</sup> min<sup>-0.5</sup>), respectively.  $C$  is a constant of IPD associated

with the thickness of the boundary layer; a higher  $C$  value indicates a greater effect of the resistance to film diffusion (larger boundary layer).

The data obtained in one-pass mode were fitted using the Yan equation (Equation (4)). Though Thomas equation is one of the most general and widely used methods in column performance theory, Yan model helps in overcoming some drawbacks associated to Thomas model, such as serious deficiency in predicting the effluent concentration during the first phase of sorption process (i.e., before and at the beginning of the breakthrough) (Yan et al., 2001). The expression is given as follows:

$$C_t = C_0 - \frac{C_0}{1 + \left(\frac{FC_0 t}{q_{ym}}\right)^{n}} \quad (4)$$

where,  $a_Y$  is the Yan model constant (dimensionless),  $q_Y$  is the maximum sorption capacity ( $\text{mg g}^{-1}$ ),  $m$  is the mass of sorbent (g),  $F$  is flow rate ( $\text{L min}^{-1}$ ) and  $t$  is the time (min),  $C_t$  and  $C_0$  are the concentrations of effluent and feed ( $\text{mg L}^{-1}$ ), respectively.

The plots of sorption isotherms were fitted by Langmuir model (Equation (5)).

$$q_{eq} = \frac{q_m b C_{eq}}{1 + b C_{eq}} \quad (5)$$

where  $b$  ( $\text{L mg}^{-1}$ ) is the affinity coefficient,  $q_m$  ( $\text{mg g}^{-1}$ ) is the sorption capacity at saturation of the monolayer in the Langmuir equation and  $q_{eq}$  ( $\text{mg g}^{-1}$ ) is the maximum sorption capacity.

All the parameters of the models were obtained by non-linear regression analysis using Origin 9.0 (Origin Lab Co., Northampton, MA, USA).

### 2.5. Pd(II) recovery from simulated leach liquors

To test the practical potential of ML/APG sponge, Pd(II) recovery from two simulated leach liquors of spent catalyst and car catalyst converter, respectively, was studied. The former liquor contains  $50 \text{ mg L}^{-1}$  of Pd(II) with 2 M of NaCl and 0.5 M of HCl (Kononova et al., 1998) and the later one has various ions including Pd(II) ( $30 \text{ mg L}^{-1}$ ), Pt(IV) ( $15 \text{ mg L}^{-1}$ ), Fe(III) ( $90 \text{ mg L}^{-1}$ ), Al(III) ( $1200 \text{ mg L}^{-1}$ ), Ce(III) ( $150 \text{ mg L}^{-1}$ ), Zn(II) ( $35 \text{ mg L}^{-1}$ ),  $\text{H}_2\text{SO}_4$  (2 M) and HCl (0.5 M) (Ricoux et al., 2017). After each batch sorption step, the sponge was washed by 20 mL pure water before continuous desorption step.

### 2.6. Characterizations

The apparent density and porosity of the sponges were measured by pycnometer measurements using ethanol as the soaking solution. The  $\text{pH}_{ZPC}$  of the sorbents were determined by the pH drift method – pH variation after contact of the sorbents with 0.1 M NaCl solutions (as the background salt) and variable initial pH. The surface functional groups were identified by Fourier transform infrared spectrophotometer (FTIR, IR Affinity-1, Shimadzu, Tokyo, Japan). X-ray photoelectron spectroscopy (XPS) measurements were carried out with a K-Alpha spectrometer (ThermoFisher Scientific, East Grinstead, UK). The morphology and microstructure of the sponges were analyzed using a field emission scanning electron microscope (FESEM, JSM-7800F & TEAM Octane Plus, JEOL, Japan) equipped with energy-dispersive X-ray spectroscopy (EDS). The element states of the samples were detected by X-ray photoelectron spectroscopy (XPS, Escalab 250, Thermo Fisher Scientific, Waltham, Massachusetts, United States).

### 2.7. Statistical analysis

Experiments were duplicated. Average values and standard deviations were calculated. The parameters of modeling were obtained by non-linear regression analysis using Origin 9.0 (Origin software Inc., San Clemente, CA, USA).

## 3. Results and discussion

### 3.1. Characterizations

By immersing the ML sponge in the alginate solution, the internal volume of the sponge can be fully filled with the biopolymer solution. This improves the dispersion of alginate-PEI all over ML sponge which forms through the ionic crosslinking between alginate and PEI (Fig. 1a). The second crosslinking between amine and aldehyde groups, forming the well-known colored Schiff bases, aims to strengthen the stability of the sponge. Alginate has been widely used as support; however, single crosslinked alginate is degraded in salty or alkaline solutions (Wang

et al., 2019). The double-crosslinking process ensures the physical and chemical stability of ALG on ML sponge in various solutions containing acids, alkalines and salts. Fig. 1b and c shows the structure of ML and ML/APG sponges, respectively. A loose network structure with large pores is observed for ML sponge. The pore size is in the range of  $166 \pm 32 \mu\text{m}$ . After modification, the sponge skeletons are homogeneously coated with APG and exhibit high roughness. The calculated loading amount of APG on ML sponge is  $73.81 \pm 0.35 \text{ wt}\%$ . The homogeneous color indicates good dispersion of ALG on ML sponge. The whole process requires no heating or specific drying processes. The simplicity, easy operation and energy saving make the process suitable for large-scale preparation of ML/APG sponge.

Fig. 1d shows the mass loss percentage of ML/APG sponges after shaking at 300 rpm for 72 h in pure water, 3 M of nitric acid, sodium hydroxide and sodium chloride, respectively. Owing to double crosslinking, ML/APG sponges are stable in various solutions containing high concentration of acid, alkaline or salt under high shaking speed with the mass loss less than 0.9%. This means the carboxyl and amine groups have been firmly wrapped on ML sponges. The inserted photos confirm this point; no particle is observed falling off from the support. The color change of ML/APG sponge from dark brown to light brown in the second solution could be due to the high protonation state of amines in strong acid. To conclude, ML/APG sponge can remain stable in complex solutions, which makes it practically applicable.

Due to the decoration of APG, the porosity inevitably decreases from 93.6% for ML to 79.9% for ML/APG sponge (Table S1, see SI). But the modified sponge is still highly porous with good percolation property. The bulk density is  $0.0086 \text{ g cm}^{-3}$  and  $0.0331 \text{ g cm}^{-3}$  for ML and ML/APG, respectively. Moreover, the  $\text{pH}_{ZPC}$  value is 6.54 for ML and 6.32 for ML/APG, meaning that in a solution at pH below these values, the surface of the sponges is positively charged and the electrostatic attraction for aqueous anions (such as chloro complexes of palladium) will play a major role in metal binding.

XPS was used to investigate surface composition of ML sponge before and after modification (Fig. 1e). As expected, the survey curve of freshly prepared materials reveals the presence of C, N, O, S and Na, which is in agreement with the composition of commercial ML sponge (Li et al., 2019a). After the modification, the peaks corresponding to Na and S disappear. This means that the surface of ML sponge has been coated by APG. Another evidence of the successful amine modification is the appearance of two new bands for N 1s (shown in Fig. S2): (a) a high binding energy ( $399.1 \text{ eV}$ ) corresponding to amine or amide groups and (b) a lower binding energy ( $398.8 \text{ eV}$ ) attributed to nitrogen in the tertiary amine groups (Ma et al., 2014). This is consistent with the characterization of PEI-GLA resins (Wang et al., 2020a), as a confirmation of the successful decoration of PEI-GLA.

The decoration of APG on melamine sponge skeletons was further characterized by FTIR-ATR spectroscopy. The spectra are shown in Fig. 1f. For ML sponge, the broad peaks observed between  $3500$  and  $3000 \text{ cm}^{-1}$  correspond to N–H stretching. The peaks at  $1541 \text{ cm}^{-1}$  and  $1320 \text{ cm}^{-1}$  represent C=N and C–N stretching vibrations of triazine ring, respectively. Peak at  $1453 \text{ cm}^{-1}$  is attributed to vibration mode of the amino group C–N–H, while  $971 \text{ cm}^{-1}$  and  $808 \text{ cm}^{-1}$  are due to the aromatic rings of ML sponge. After decoration with APG, the intensity of these peaks decreases obviously, again, indicating that the surface of ML has been mostly coated with APG. The peak at  $1590 \text{ cm}^{-1}$  is due to the formation of C=N bonds (Li et al., 2019b). This peak is commonly found for materials with “Schiff’s base” formed by the reaction between PEI and GA (Hu et al., 2019). The peak at  $1396 \text{ cm}^{-1}$  can be assigned to  $\text{COO}^-$  symmetric stretching of the carboxylate groups in alginate, while the one at  $1031 \text{ cm}^{-1}$  represents C–O asymmetric stretching (Ren et al., 2017).

Despite several tries, it was not possible evaluating the textural properties of the material. This is probably to the large size of the pores that makes imprecise the determination of specific surface area.

### 3.2. The improvement of modification on Pd(II) sorption

The comparison of raw ML sponge and modified sponge for Pd(II) sorption is illustrated in Fig. S3. Judging from the asymptotic trend of uptake found in Pd(II) sorbed by the sponges, the Freundlich equation, which has an exponential form (power-type function), is apparently not suitable for fitting the sorption isotherms. Langmuir predicts well the data obtained by both sorbents and the parameters shown in Table S2 suggest a  $R^2$  of 0.83 for ML and 0.95 for ML/APG sponges. The maximum sorption capacity calculated is  $9.7 \text{ mg g}^{-1}$  for ML and  $134.3 \text{ mg g}^{-1}$  for ML/APG sponge. This means the functionalization of ML sponge has dramatically improved the sorption performance for Pd(II). It is noted that the loading amount of APG on ML sponge is  $73.81 \pm 0.35 \text{ wt\%}$ . This means the sorption capacity of APG for Pd(II) is as high as  $168.8 \text{ mg g}^{-1}$ , when referred to the amount of coating. Such improvement on sorption of Pd(II) is obviously attributed to the introduction of amine groups on APG. Indeed, Demadis et al. (2011) reported the values of pKa for primary, secondary and tertiary amines of PEI: 4.5, 6.7 and 11.6, respectively. This means that in acidic solutions the amines are uniformly protonated and then able to bind chloro-anionic palladium species. Table S3 (see SI) reports Pd(II) sorption properties for a variety of materials. In general, phenolic hydroxyl group-based and carboxyl-based materials such as tannin (Can et al., 2013), moss (Sari et al., 2009), and alginate (da Silva et al., 2021) show the lowest sorption capacity among the listed materials. Silica-based isoBu-BTP/SiO<sub>2</sub>-P (Ning et al., 2020) and WS<sub>2</sub> (Wang et al., 2020b) microcrystals The raw chitosan (Nagireddi et al., 2017) that contains a certain amount of amine groups shows much higher sorption capacity. Aminated alginate (Gao et al., 2020; Cataldo et al., 2015), algal biomass beads (Wang et al., 2018), ionic liquid modified chitosan (Kumar et al., 2015) and amine-rich metal-organic frameworks (Chen et al., 2021; Lim et al., 2020) possess the highest sorption capacities. Although ML/APG sponge only has a moderate sorption capacity in the listed materials, its specific form (porous sponge) and high stability in solutions with a large range of pH values make it more flexible for operation. Moreover, most studies showed that it requires more than 24 h for Pd(II) sorption equilibrium onto PEI-functionalized alginate materials (Wei et al., 2021; Wang et al.,

2017a), while it only takes less than 450 min for ML/APG (see below). This means that coating the materials onto ML sponge, to some degree, decreases Pd(II) diffusion resistance. These properties make it attractive for practical application.

### 3.3. Comparison of recirculation and one-pass modes

#### 3.3.1. Sorption

It is well-known that the sorption kinetic is normally controlled by resistance to external diffusion (or so-called film diffusion), surface diffusion, pore diffusion, or a combination of surface and pore diffusion. FR is a way to simulate batch system. A higher flow rate is in favor of reducing the resistance to film/intraparticle diffusion and thus increases the sorption kinetics. By contrast, a higher flow rate for FO normally results in a small retention time, which causes a smaller breakthrough point and a lower sorption efficiency. Therefore, to obtain a better sorption performance for both modes, we applied different flow rates (i. e.,  $10 \text{ mL min}^{-1}$  and  $50 \text{ mL min}^{-1}$  for FR and  $1 \text{ mL min}^{-1}$  and  $5 \text{ mL min}^{-1}$  for FO) for the comparison of sorption kinetics and the results are shown in Fig. 2a and b, respectively. The profiles in Fig. 2a indicate that high flow rate slightly enhances sorption kinetics under FR: hence, the equilibrium is achieved within 450 min and 300 min at  $10 \text{ mL min}^{-1}$  and  $50 \text{ mL min}^{-1}$ , respectively. The curves can be better fitted by PSORE compared to PFORE. The apparent rate constant of Pd(II) sorption calculated from PSORE (shown in Table S4) supports the above results with a value of  $3.60 \times 10^{-4} \text{ g mg}^{-1} \text{ min}^{-1}$  at  $10 \text{ mL min}^{-1}$ , smaller than  $6.50 \times 10^{-4} \text{ g mg}^{-1} \text{ min}^{-1}$  at  $50 \text{ mL min}^{-1}$ , further demonstrating the faster kinetic at higher flow rate. However, the equilibrium sorption capacities at these two flow rates show almost no difference. Although PSORE can adequately predict the sorption kinetics, it fails to suggest the sorption mechanisms, while the intraparticle diffusion model (IPD) can identify the sorption pathways and reveal the rate-controlling step. Fig. S4 presents the plot of  $q_t$  against  $t^{0.5}$ . Two main stages before achieving equilibrium can be identified. The first one refers to the sorption step controlled by the resistance to surface diffusion. During this step, a large amount of Pd(II) is attached to the sorption sites that are readily accessible. The second stage represents the mass transfer

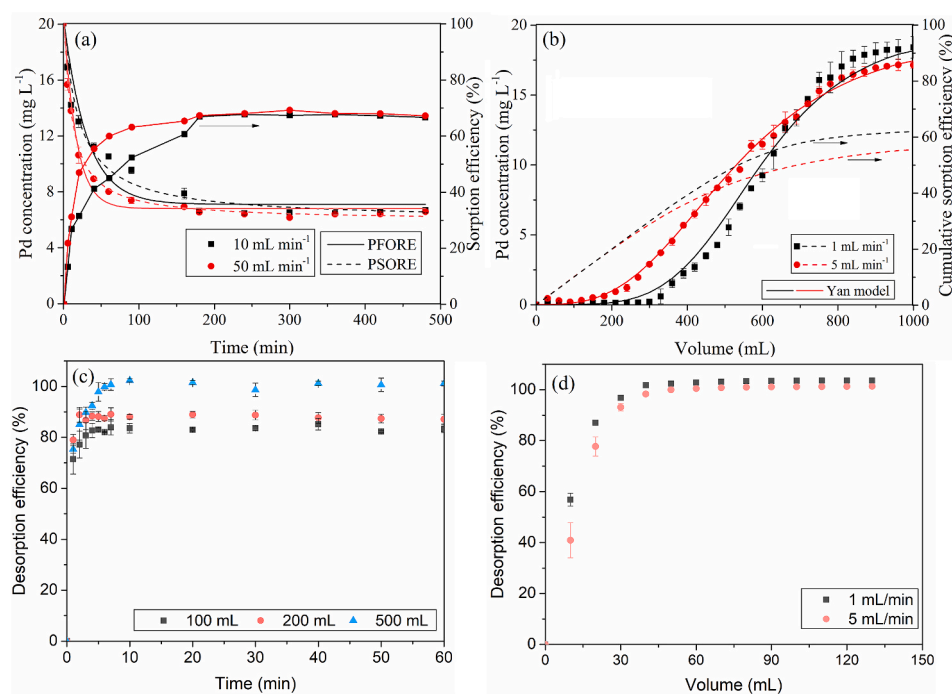


**Fig. 2.** Sorption of Pd(II) under (a) FR and (b) FO; desorption of Pd(II) under (c) FR and (d) FO (For sorption: Pd(II) concentration =  $20 \text{ mg L}^{-1}$ , sponge mass = 100 mg, pH = 1 adjusted using HCl and volume = 1L; for desorption: sponge mass = 100 mg, Pd(II)-loaded amount  $\approx 120 \text{ mg g}^{-1}$ , flow rate under FR =  $50 \text{ mL min}^{-1}$ ).

controlled by the resistance to intraparticle diffusion, during which, the sorption rate is much slower than that at the first stage ( $k_{id,2} < k_{id,1}$  shown in Table S4). A higher flow rate can improve diffusion properties at both stages.

For FO, the flow rate also plays an important role. A higher flow rate normally results in a small retention time, which causes a smaller breakthrough point and a lower sorption efficiency. On the other hand, a low flow rate can provide sufficient contact time and thus improves the sorption efficiency, but this requires a longer processing time. As shown in Fig. 2b, when the flow rate decreases from 5 to 1 mL min<sup>-1</sup>, the breakthrough point increases from 90 mL to 180 mL and the cumulative sorption capacity grew from 107.4 to 114.4 mg g<sup>-1</sup> when passing 1 L of feed solution. The result is opposite to the study of Pb(II) sorption onto alginate foams (Wang et al., 2017b), which was hardly affected by flow rate owing to easy diffusion of Pb(II) into porous structure of alginate foams. One reason could be the larger size of chloro-palladium complex (ionic radius PdCl<sub>4</sub><sup>2-</sup> = 2.75, Pb(II) = 1.21 (Shannon, 1976)) which makes it more difficult to diffuse into the sorption sites. Moreover, although the double crosslinking makes the structure highly stable, it inevitably increases the resistance to intra-particle diffusion (Zhang et al., 2019a) and thus prolongs the required residue time for Pd(II) sorption. Zhang et al. (2019b) also reported a similar phenomenon with the present study that a higher flow rate decreased U(VI) uptake due to insufficient residence time. The result means that a smaller flow rate can reduce the amount of feed solution to achieve the equilibrium. Indeed, the fitting curves by Yan model ( $R^2 > 0.99$ ) show that to reach the equilibrium, it requires 1.8 L at 1 mL min<sup>-1</sup>, while that is more than 5 L at 10 mL min<sup>-1</sup>. Under FR, it only requires 0.7 L (Fig. S5), which allows reaching a higher removal efficiency using the same amount of sorbent and a high concentration factor in the following elution step. The sorption efficiency under FR is more than 65%, regardless of flow rate, while that under FO does not exceed 60%. The same trend is observed when the inlet Pd(II) concentration is lower (Fig. S6): FO requires a much slower flow rate to get a higher sorption efficiency (90% at 1 mL min<sup>-1</sup> and 85% at 5 mL min<sup>-1</sup>) and thus a much longer operating time, while almost 97% sorption efficiency is achieved within 300 min under FR with a flow rate of 50 mL min<sup>-1</sup>.

### 3.3.2. Desorption

Desorption is essential for the design of sorption-based technology. Metal elution contributes to (a) concentrating target contaminants and (b) reusing spent sorbents. Experiments were firstly conducted under FR using 0.1 M HCl, 0.025 M thiourea and a mixture of 0.1 M HCl and 0.025 M thiourea to confirm the choice of eluting agent. Result (shown in Fig. S7) confirms the best desorption performance of acidic thiourea, which is in agreement with previous studies (Wei et al., 2021; Li et al., 2019c). It was then used for the comparison of Pd(II) desorption under FR and FO.

Different volumes of HCl/thiourea solution were used for Pd(II) desorption under FR. Complete desorption (100%) can be obtained when using 500 mL of desorption reagent, while 100 mL or 200 mL volumes only achieve less than 90% desorption efficiency (shown in Fig. 2c). However, a large volume of desorption reagent will cause a smaller CF. Under FO, nearly 100% of desorption has been achieved at 40 mL at flow rate of 1 mL min<sup>-1</sup> (shown in Fig. 2d). The time used is 40 min, longer than that under FR; however, the CF values are 38, 22, and 7 for the first, second and third 10 mL-volumes of the eluent, much higher than those reported under FR (CF = 0.5–5). The values are also higher than one of our previous studies, in which, the CF values were in the range of 7.9–8.4, 7.8–8.1 and 4.2–6.3 for alginate, algal biomass (AB) and AB/PEI discs, respectively, under FR (Wang et al., 2017c). The results confirm the advantage of desorption under FO over FR.

### 3.4. Pd sorption mechanism

Based on the literature, the sorption of Pd(II) by functionalized

materials may involve electrostatic attraction, coordination and ion exchange. However, the predominant sorption mechanism strongly depends on the experimental conditions (i.e., solution pH, temperature, etc.), sorbate characteristics (species, pK<sub>a</sub>, etc.) and sorbent properties (pH<sub>ZPC</sub>, surface area, functional groups, etc.). Solution pH affects both the species of aqueous Pd(II) and the chemical state (protonation or deprotonation) of functional groups; it is considered as one of the most important factors in Pd(II) sorption process. Therefore, the sorption mechanism of Pd(II) was firstly discussed through the study of pH effect (Fig. 3a). The effect of pH has been investigated under FR using H<sub>2</sub>SO<sub>4</sub> and HCl for pH adjustment in the range of pH0.5 to pH2, respectively. To ensure no formation of precipitable PdO, higher pH values were not studied (da Silva et al., 2021). The speciation of Pd(II) species shows the predominance of chloro-palladium complexes when using HCl for pH control (Fig. 3b). The percentage of PdCl<sub>4</sub><sup>2-</sup> increased from 63% at pH 2–97% at pH 1 and the sorption capacity increased from 87 mg g<sup>-1</sup> at pH 2–127 mg g<sup>-1</sup> at pH 1. Ricoux et al. (2015) also reported an increase in Pd(II) sorption capacity onto functionalized polymer with increasing pH. They concluded that Pd(II) sorption mainly involved ligand exchange mechanisms; the decreasing pH resulted in protonation of amine groups and thus limited the coordination of Pd(II). The opposite result of this study means a different sorption mechanism: electrostatic attraction between protonated amines and chloro-anionic complexes. Indeed, pH decreasing from pH 2 to pH 1 leads to a higher percentage of chloro-anionic complexes (i.e., PdCl<sub>4</sub><sup>2-</sup> and PdCl<sub>3</sub><sup>-</sup>) in HCl-adjusted solution and higher level of protonation of amines, but also a higher competition effect of chloride anions for binding on protonated amine groups. This is the first evidence that the primary mechanism of Pd(II) sorption onto ML/APG is the electrostatic attraction between protonated amines and chloro-anionic complexes. In the case of H<sub>2</sub>SO<sub>4</sub>-adjusted solutions, the concentration of chloro-anionic complexes is much lower and the sorption capacity significantly reduces. The uptake for Pd(II) at pH 0.5 is the lowest regardless of pH adjuster; this can be attributed to the strong competition of Cl<sup>-</sup> or SO<sub>4</sub><sup>2-</sup> in strong acidic solutions. Besides amines, carboxyl groups could also play a role in Pd(II) binding (Rasoulzadeh et al., 2021). It has been reported that when the pH was higher than pK<sub>a</sub> values of carboxyl groups (i.e., 3.38 and 3.65 for mannuronic and guluronic acids, respectively), the deprotonation of carboxylic acid groups allowed the complexation of metal cations (Pd<sup>2+</sup> or PdCl<sup>+</sup>). Considering the low pH used in the present study, carboxyl groups are highly protonated and the complexation mechanism is strongly limited. Element mapping (Fig. 3c) shows that the distribution of Pd is correlated to that of Cl element; this, to some degree, further demonstrates that Pd(II) has been loaded under the forms of chloro-anionic metal complexes.

The binding mechanism was then studied by FTIR analysis (Fig. 3d). After Pd(II) sorption, the shift of the band attributed to amine groups confirms that the groups played an important role. However, the disappearance of the band corresponding to carboxyl groups is a surprise. Indeed, based on previous discussion, they should not be involved in metal binding. The disappearance of the band could be due to two reasons: 1) the reaction of the groups with chemicals, leading to the formation of new functional groups; 2) the protonation of carboxyl groups resulting in the band shifting and overlapping with another band. Since the solution only contains PdCl<sub>2</sub> and HCl, the former reason can be eliminated. The peak at 1453 cm<sup>-1</sup>, corresponding to vibration mode of the amino C–N–H, become wider and its intensity also increases slightly. This could be due to the overlapping of symmetric stretching vibrations of carboxylate groups (Wang et al., 2020a), which is a support for the latter reason.

To verify the uptake and the valence state of the Pd, XPS analysis was performed (Fig. 3e). The characteristic peaks (Fig. 3f) of binding energies at 338 eV and 344 eV for Pd 3d<sub>5/2</sub> and Pd 3d<sub>3/2</sub>, respectively, confirm the oxidation state of Pd is +2. The appearance of Cl element again verifies the loading of chloro-anionic Pd species on the sorbent. Moreover, a third band at 400.2 eV (shown in Fig. S8) associated with N

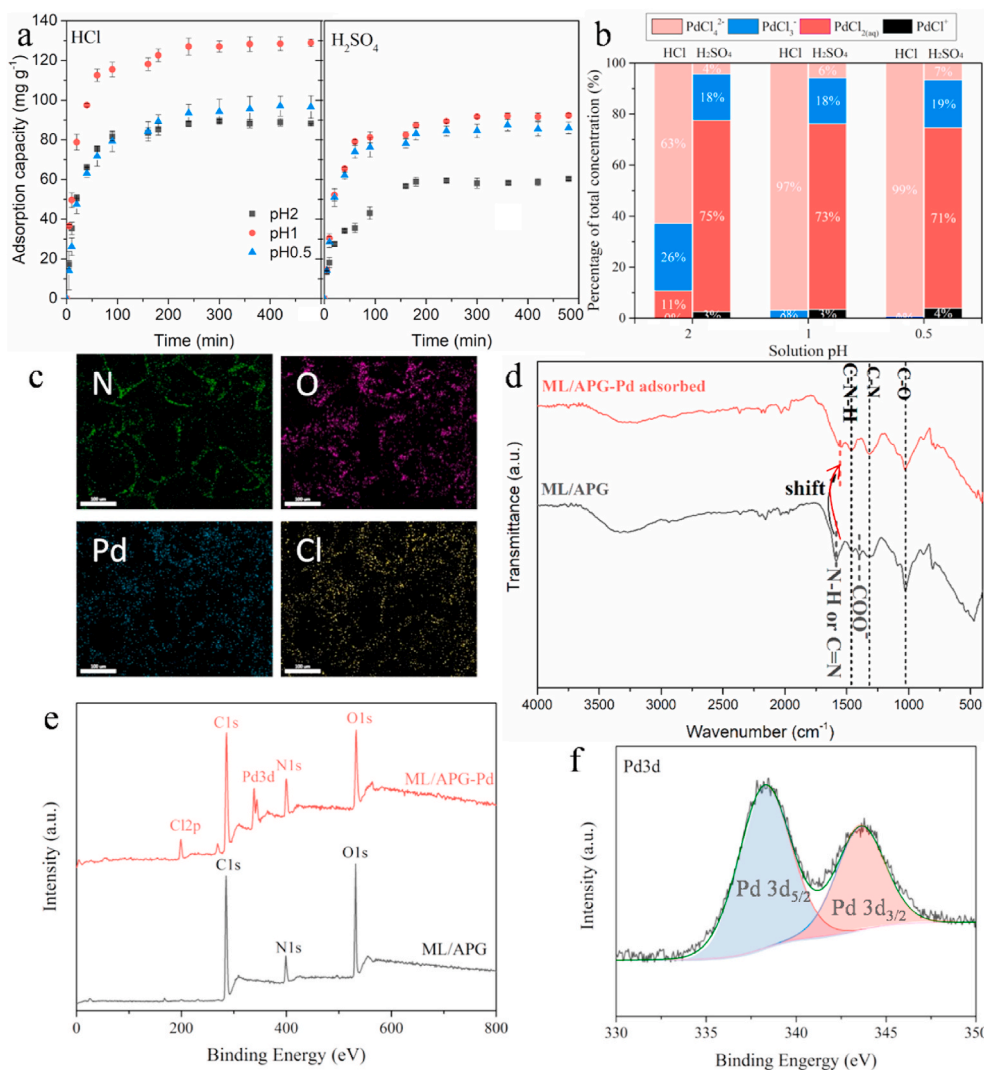


**Fig. 3.** (a) Effect of pH adjuster and pH values on Pd(II) sorption; (b) Pd(II) speciation at different pHs adjusted by H<sub>2</sub>SO<sub>4</sub> or HCl; (c) FTIR spectra of ML/APG and Pd-loaded ML/APG; (e) XPS survey analysis and (f) Pd 3d spectra for Pd-loaded ML/APG.

element appears as the bond between N and Pd (Wang et al., 2020c), further demonstrating the reaction between amine groups and chloro-anionic Pd species. It is noteworthy that a new band at 289.1 eV for C 1s appears. This probably means that the strongly acidic medium affects the chemical environment of carboxyl groups by forming carboxylic acid. Accordingly, a new band at 534.6 eV assigned to C-OH (Yadav et al., 2020) is also observed for O1s.

### 3.5. Reuse of sponge for Pd(II) concentration

The above desorption experiment has confirmed the high efficiency of acidic thiourea as the eluent solution for Pd(II) recovery. The reusability of ML/APG sponge and Pd(II) recovery from low-concentration solution were studied by combining FR for sorption step and FO for elution step. Fig. 4 shows the sorption and desorption efficiencies for 10 successive cycles. The sorption efficiency is more than 96% after 100 min of reaction. Interestingly, the sorption kinetic increases slightly at the third cycle; this could be due to the presence of 0.025 M thiourea in the eluent solution, which gradually chemically modifies the surface functional groups of the sponge. Indeed, the FTIR spectra of raw and reused ML/APG sponges (shown in Fig. S9) show a new small peak at 1396 cm<sup>-1</sup>, corresponding to stretching vibration of C=S (Chen et al., 2020; Cai et al., 2019). The elution performance under FO was stable

with a 100% desorption efficiency after passing 50 mL eluent solution. The concentration factor (CF, ratio of metal concentration in the eluate over its concentration in the sorption used for sorption), shown in Fig. S10, was above or close to 70 for the first 10 mL-sample and much more than 40 for the second 10 mL-sample. Moreover, SEM images (shown in Fig. S11) of the sponges after Pd-loaded and 10 cycles show that APG is firmly attached on ML sponge after sorption and desorption. The high CF and good mechanical and chemical stability during 10 cycles confirm the high potential of ML/APG sponge for practical application in Pd(II) recovery from acidic solutions.

### 3.6. Pd(II) recovery from simulated leach liquors

The above results have confirmed the high efficiency of the combined process involving batch sorption and fixed-bed elution for Pd(II) recovery. This section aims to evaluate the application potential of such system for recovering Pd(II) from synthesized leaching liquors using ML/APG sponge.

Fig. 5a shows that the sorption efficiency of the sponge for Pd(II) decreases significantly: the sorption efficiency is around 80% when the dose is 1 g L<sup>-1</sup>, which is due to the presence of chloride ions in excess. A 96% sorption efficiency can be achieved when the dose increases to 2 g L<sup>-1</sup>. Using 60 mL of acidic thiourea as the desorption agent, more than

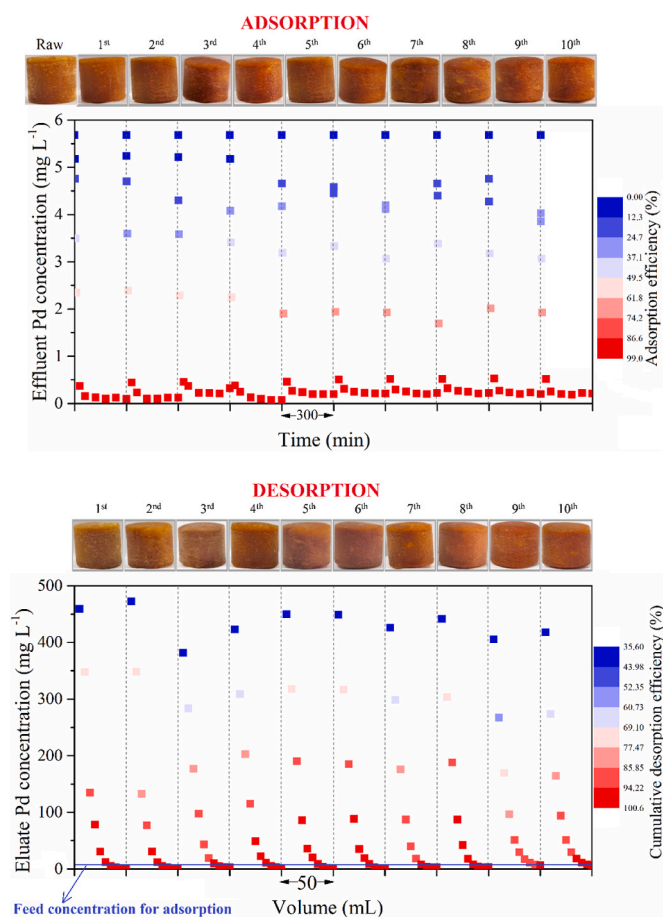


**Fig. 4.** Reuse of ML/APG sponge for Pd(II) concentration (For sorption: volume = 1 L, Pd(II) concentration = 5.7 mg L<sup>-1</sup>, flow rate = 50 mL min<sup>-1</sup>, pH = 1.0 adjusted using HCl; For elution: flow rate = 1 mL min<sup>-1</sup>).

87% (cumulative desorption efficiency) of Pd(II) can be desorbed. The Pd(II) concentration in the first 5 mL of effluent is as high as 1178, 897 in the second, and 554 mg L<sup>-1</sup> in the third. The corresponding CF values are 23.7, 18.0 and 11.1, respectively.

Fig. 5b presents the result of Pd(II) recovery from the leachate of the catalytic converter. The concentration of Pd(II) and Pt(IV) decreases from 28.6 to 12.9 mg L<sup>-1</sup> to 3.40 and 4.58 mg L<sup>-1</sup>, respectively. However, the sorption of Al(III), Fe(III), Ce(III) or Zn(II) remains negligible. The dominant presence of Pd(II) in the eluent solutions indicates the selectivity of ML/APG sponge for Pd(II) over Pt(IV) and other metal cations. The CF value is 19.5 for Pd(II) > 14.2 for Pt(IV) ≫ 0.80 for Fe

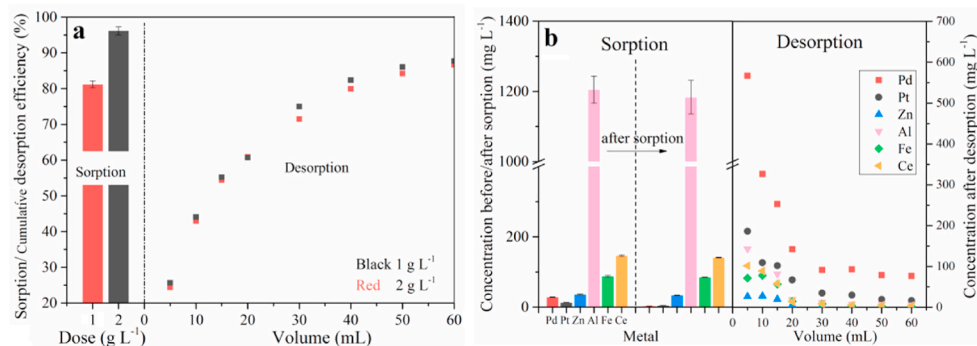


**Fig. 5.** Pd(II) recovery from synthesized leachates of spent (a) catalysts (Batch sorption step: V: 0.5 L; mass: 0.5 g or 1.0 g; time: 72 h; flow rate: 50 mL min<sup>-1</sup>—continuous desorption step: 0.1 M HCl/0.025 M Thiourea solution; flow rate: 1 mL min<sup>-1</sup>); and (b) car catalyst converter (Batch sorption step: V: 0.5 L; mass: 1.0 g; time: 72 h; flow rate: 50 mL min<sup>-1</sup>—continuous desorption step: 0.1 M HCl/0.025 M Thiourea solution; flow rate: 1 mL min<sup>-1</sup>).

(III) ≈ 0.75 for Zn(II) ≈ 0.69 for Ce(III) > 0.12 for Al(III). This means a high selectivity of ML/APG sponge for Pd(II) over other metals.

To conclude, ML/APG can be successfully applied in acidic solutions for Pd(II) recovery. Although the presence of coexisting ions negatively affects its sorption performance, the high stability, good operation flexibility (applicable in different modes) and high selectivity over metal cations still make it promising for practical application as reusable sorbents.

#### 4. Conclusions and prospects

This study compared fixed-bed recirculation mode (FR, simulating batch system) and one-pass mode (FO) for Pd(II) sorption and elution using alginate/PEI-GA melamine (ML/APG) sponge. Results show that the coated polymeric materials on ML sponge are stable when exposed to highly acidic or alkaline media. The amine-functionalization significantly improve its sorption affinity towards Pd(II) in acidic solutions. FR maximizes the utilization of the sorbent, while FO minimize the required volume of eluent solution for metal desorption. The combined process of FR for sorption and FO enables the efficient concentration of Pd(II). In addition, ten cycles of sorption-elution demonstrated the high stability of the sponge in terms of both sorption and desorption and also that this combination allows reaching high concentration factor for Pd(II) recovery from synthesized leach liquors of spent catalysts.

The high stability and good sorption affinity for Pd(II) of ML/APG sponge have been certified in this study. Further studies can focus on the possibility of using this sponge as support for catalytic metals (heterogeneous catalysis) by binding Pd(II). Post-reduction (with chemical agent) will help in designing green supported catalysts. In addition, to this application in heterogeneous catalysis, the concept tested with Pd(II) could be extended to other valuable metals having similar chemistry (formation of metal anions), such as Pt(IV), Au(III), etc. The functionalization of amine groups with specific grafting of new reactive groups (amidoximation, phosphonation, sulfonation, etc.) would bring new reactive functions, opening other applications for the recovery of valuable metals, combining with the superior properties of these materials in terms of hydrodynamics (free gravity percolation).

#### CRedit authorship contribution statement

**Chuande Yu:** Conducting a research and investigation process, Data curation. **Zhaojiang Wu:** Writing – original draft. **Shengye Wang:** Provision of study materials. **Qilong Zhong:** Validation. **Bo Yang:** Project administration. **Jiajie Xu:** Data presentation. **Ke Xiao:** Supervision. **Eric Guibal:** Writing - review & editing.

## Declaration of competing interest

The authors declare that they have no known competing financial interests or personal relationships that could have appeared to influence the work reported in this paper.

## Acknowledgements

The authors thank the National Natural Science Foundation of China (22178222), and the Guangdong Basic and Applied Basic Research Foundation (2021A1515010540) for providing financial support.

## References

- Cai, W., Zhu, F., Liang, H., Jiang, Y., Tu, W., Cai, Z., Wu, J., Zhou, J., 2019. Preparation of thiourea-modified magnetic chitosan composite with efficient efficiency for Cr(VI). *Chem. Eng. Res. Des.* 144, 150–158. <https://doi.org/10.1016/j.cherd.2019.01.031>.
- Can, M., Bulut, E., Ornek, A., Ozacar, M., 2013. Synthesis and characterization of valonea tannin resin and its interaction with palladium (II), rhodium (III) chloro complexes. *Chem. Eng. J.* 221, 146–158. <https://doi.org/10.1016/j.cej.2013.01.043>.
- Cataldo, S., Muratore, N., Orecchio, S., Pettignano, A., 2015. Enhancement of adsorption ability of calcium alginate gel beads towards Pd (II) ion. A kinetic and equilibrium study on hybrid Laponite and Montmorillonite–alginate gel beads. *Appl. Clay Sci.* 118, 162–170. <https://doi.org/10.1016/j.clay.2015.09.014>.
- Chen, X., Xiang, Y., Xu, L., Liu, G., 2020. Recovery and reduction of Au(III) from mixed metal solution by thiourea-resorcinol-formaldehyde microspheres. *J. Hazard Mater.* 397, 122812. <https://doi.org/10.1016/j.jhazmat.2020.122812>.
- Chen, M., Li, S., Jin, C., Shao, M., Huang, Z., Xie, X., 2021. Removal of metal-cyanide complexes and recovery of Pt (II) and Pd (II) from wastewater using an alkali-tolerant metal-organic resin. *J. Hazard Mater.* 406, 124315. <https://doi.org/10.1016/j.jhazmat.2020.124315>.
- da Silva, T.L., da Silva, M.G.C., Vieira, M.G.A., 2021. Palladium adsorption on natural polymeric sericin-alginate particles crosslinked by polyethylene glycol diglycidyl ether. *J. Environ. Chem. Eng.* 105617 <https://doi.org/10.1016/j.jece.2021.105617>.
- Demadis, K.D., Paspalaki, M., Theodorou, J., 2011. Controlled release of bis (phosphonate) pharmaceuticals from cationic biodegradable polymeric matrices. *Ind. Eng. Chem. Res.* 50, 5873–5876. <https://doi.org/10.1021/ie102546g>.
- Duman, O., Diker, C.Ö., Tunc, S., 2021. Development of highly hydrophobic and superoleophilic fluoro organothiol-coated carbonized melamine sponge/rGO composite adsorbent material for the efficient and selective absorption of oily substances from aqueous environments. *J. Environ. Chem. Eng.* 9, 105093. <https://doi.org/10.1016/j.jece.2021.105093>.
- Gao, X., Guo, C., Hao, J., Zhao, Z., Long, H., Li, M., 2020. Selective adsorption of Pd (II) by ion-imprinted porous alginate beads: experimental and density functional theory study. *Int. J. Biol. Macromol.* 157, 401–413. <https://doi.org/10.1016/j.ijbiomac.2020.04.153>.
- Gao, C., Wang, X.-L., An, Q.-D., Xiao, Z.-Y., Zhai, S.-R., 2021. Synergistic preparation of modified alginate aerogel with melamine/chitosan for efficiently selective adsorption of lead ions. *Carbohydr. Polym.* 256, 117564. <https://doi.org/10.1016/j.carbpol.2020.117564>.
- García, A., Deyris, P.-A., Adler, P., Pelissier, F., Dumas, T., Legrand, Y.-M., Grison, C., 2021. I-Ecologically responsible and efficient recycling of Pd from aqueous effluents using biosorption on biomass feedstock. *J. Clean. Prod.* 299, 126895. <https://doi.org/10.1016/j.jclepro.2021.126895>.
- Hu, D., Jiang, R., Wang, N., Xu, H., Wang, Y.-G., Ouyang, X.-k., 2019. Adsorption of diclofenac sodium on bilayer amino-functionalized cellulose nanocrystals/chitosan composite. *J. Hazard Mater.* 369, 483–493. <https://doi.org/10.1016/j.jhazmat.2019.02.057>.
- Kononova, O., Kholmogorov, A., Mikhlina, E., 1998. Palladium sorption on vinylpyridine ion exchangers from chloride solutions obtained from spent catalysts. *Hydrometallurgy* 48, 65–72. [https://doi.org/10.1016/S0304-386X\(97\)00062-5](https://doi.org/10.1016/S0304-386X(97)00062-5).
- Kumar, A.S.K., Sharma, S., Reddy, R.S., Barathi, M., Rajesh, N., 2015. Comprehending the interaction between chitosan and ionic liquid for the adsorption of palladium. *Int. J. Biol. Macromol.* 72, 633–639. <https://doi.org/10.1016/j.ijbiomac.2014.09.002>.
- Li, M., Bian, C., Yang, G., Qiang, X., 2019a. Facile fabrication of water-based and non-fluorinated superhydrophobic sponge for efficient separation of immiscible oil/water mixture and water-in-oil emulsion. *Chem. Eng. J.* 368, 350–358. <https://doi.org/10.1016/j.cej.2019.02.176>.
- Li, J., Yuan, S., Zhu, J., Van der Bruggen, B., 2019b. High-flux, antibacterial composite membranes via polydopamine-assisted PEI-TiO<sub>2</sub>/Ag modification for dye removal. *Chem. Eng. J.* 373, 275–284. <https://doi.org/10.1016/j.cej.2019.05.048>.
- Li, S., Chu, N., Li, X., Dong, F., Shen, Y., 2019c. Recovery of palladium from acidic nitrate media with triazole type extractants in ionic liquid. *Hydrometallurgy* 189, 105148. <https://doi.org/10.1016/j.hydromet.2019.105148>.
- Li, S., Yang, F., Zhang, Y., Lan, Y., Cheng, K., 2021. Performance of lead ion removal by the three-dimensional carbon foam supported nanoscale zero-valent iron composite. *J. Clean. Prod.* 294, 125350. <https://doi.org/10.1016/j.jclepro.2020.125350>.
- Lim, C.-R., Lin, S., Yun, Y.-S., 2020. Highly efficient and acid-resistant metal-organic frameworks of ML-101 (Cr)-NH<sub>2</sub> for Pd(II) and Pt(IV) recovery from acidic solutions: adsorption experiments, spectroscopic analyses, and theoretical computations. *J. Hazard Mater.* 387, 121689. <https://doi.org/10.1016/j.jhazmat.2019.121689>.
- Ma, Y., Liu, W.-J., Zhang, N., Li, Y.-S., Jiang, H., Sheng, G.-P., 2014. Polyethylenimine modified biochar adsorbent for hexavalent chromium removal from the aqueous solution. *Bioresour. Technol.* 169, 403–408. <https://doi.org/10.1016/j.biortech.2014.07.014>.
- Nagireddi, S., Katiyar, V., Uppaluri, R., 2017. Pd(II) adsorption characteristics of glutaraldehyde cross-linked chitosan copolymer resin. *Int. J. Biol. Macromol.* 94, 72–84. <https://doi.org/10.1016/j.ijbiomac.2016.09.088>.
- Ning, S., Zhang, S., Zhang, W., Zhou, J., Wang, S., Wang, X., Wei, Y., 2020. Separation and recovery of Rh, Ru and Pd from nitrate solution with a silica-based IsoBu-BTP/SiO<sub>2</sub>-P adsorbent. *Hydrometallurgy* 191, 105207. <https://doi.org/10.1016/j.hydromet.2019.105207>.
- Niu, H., Li, J., Qiang, Z., Ren, J., 2021. Versatile and cost-efficient cleanup of viscous crude oil by elastic carbon sorbent from direct pyrolysis of melamine foam. *J. Mater. Chem. A* 9 (18), 11268–11277. <https://doi.org/10.1039/D1TA01133B>.
- Pinto, J., Lopes, C.B., Henriques, B., Couto, A.F., Ferreira, N., Carvalho, L., Costa, M., Torres, J.M., Vale, C., Pereira, E., 2021. Platinum-group elements sorption by living macroalgae under different contamination scenarios. *J. Environ. Chem. Eng.* 9, 105100. <https://doi.org/10.1016/j.jece.2021.105100>.
- Prasetyo, E., Anderson, C., 2020. Platinum group elements recovery from used catalytic converters by acidic fusion and leaching. *Metals-Basel* 10, 485. <https://doi.org/10.3390/met10040485>.
- Rasoulzadeh, H., Sheikhmohammadi, A., Abtahi, M., Roshan, B., Jokar, R., 2021. Eco-friendly rapid removal of palladium from aqueous solutions using alginate-diatomite magnanone composite. *J. Environ. Chem. Eng.* 105954. <https://doi.org/10.1016/j.jece.2021.105954>.
- Ren, J., Musyoka, N.M., Langmi, H.W., North, B.C., Mathe, M., Pang, W., Wang, M., Walker, J., 2017. In-situ IR monitoring of the formation of Zr-fumarate MOF. *Appl. Surf. Sci.* 404, 263–267. <https://doi.org/10.1016/j.apsusc.2017.01.271>.
- Ricoux, Q., Bocokić, V., Méricq, J.P., Bouyer, D., Zutphen, S.V., Faur, C., 2015. Selective recovery of palladium using an innovative functional polymer containing phosphine oxide. *Chem. Eng. J.* 264, 772–779. <https://doi.org/10.1016/j.cej.2014.11.139>.
- Ricoux, Q., Méricq, J., Bouyer, D., Bocokić, V., Hernandez-Juarez, L.C., Zutphen, S.V., Faur, C., 2017. A selective dynamic sorption-filtration process for separation of Pd (II) ions using an aminophosphine oxide polymer. *Separ. Purif. Technol.* 174, 159–165. <https://doi.org/10.1016/j.seppur.2016.10.025>.
- Sari, A., Mendil, D., Tuzen, M., Soylak, M., 2009. Biosorption of palladium(II) from aqueous solution by moss (*Racomitrium lanuginosum*) biomass: equilibrium, kinetic and thermodynamic studies. *J. Hazard Mater.* 162, 874–879. <https://doi.org/10.1016/j.jhazmat.2008.05.112>.
- Shannon, R.D., 1976. Revised effective ionic radii and systematic studies of interatomic distances in halides and chalcogenides. *Acta Crystallogr.* 32, 751–767. <https://doi.org/10.1107/S0567739476001551>.
- Wang, S., Vincent, T., Roux, J.-C., Faur, C., Guibal, E., 2017a. Pd (II) and Pt (IV) sorption using alginate and algal-based beads. *Chem. Eng. J.* 313, 567–579. <https://doi.org/10.1016/j.cej.2016.12.039>.
- Wang, S., Vincent, T., Faur, C., Guibal, E., 2017b. Algal foams applied in fixed-bed process for lead(II) removal using recirculation or one-pass modes. *Mar. Drugs* 15, 315. <https://doi.org/10.3390/md15100315>.
- Wang, S., Vincent, T., Roux, J.-C., Faur, C., Guibal, E., 2017c. Innovative conditioning of algal-based sorbents: macro-porous discs for palladium sorption. *Chem. Eng. J.* 325, 521–532. <https://doi.org/10.1016/j.jece.2017.05.103>.
- Wang, S., Vincent, T., Faur, C., Guibal, E., 2018. A comparison of palladium sorption using polyethylenimine impregnated alginate-based and carrageenan-based algal beads. *Appl. Sci.* 8 (2), 264. <https://doi.org/10.3390/app8020264>.
- Wang, S., Vincent, T., Faur, C., Rodríguez-Castellón, E., Guibal, E., 2019. A new method for incorporating polyethylenimine (PEI) in algal beads: high stability as sorbent for palladium recovery and supported catalyst for nitrophenol hydrogenation. *Mater. Chem. Phys.* 221, 144–155. <https://doi.org/10.1016/j.matchemphys.2018.09.021>.
- Wang, S., Xiao, K., Mo, Y., Yang, B., Vincent, T., Faur, C., Guibal, E., 2020a. Selenium(VI) and copper(II) adsorption using polyethylenimine-based resins: effect of glutaraldehyde crosslinking and storage condition. *J. Hazard Mater.* 386, 121637. <https://doi.org/10.1016/j.jhazmat.2019.121637>.
- Wang, L., Wang, K., Huang, R., Qin, Z., Su, Y., Tong, S., 2020b. Hierarchically flower-like WS<sub>2</sub> microcrystals for capture and recovery of Au(III), Ag(I) and Pd(II). *Chemosphere* 252, 126578. <https://doi.org/10.1016/j.chemosphere.2020.126578>.
- Wang, S., Mo, Y., Vincent, T., Roux, J.-C., Rodríguez-Castellón, E., Faur, C., Guibal, E., 2020c. Palladium nanoparticles supported on amine-functionalized alginate foams for hydrogenation of 3-nitrophenol. *J. Mater. Sci.* 55, 2032–2051. <https://doi.org/10.1007/s10853-019-04099-y>.
- Wei, W., Qiu, Y., Zhao, Y., Zhang, K., Ji, Y., Gao, H., Bediako, J.K., Yun, Y.-S., 2021. Development of melamine-impregnated alginate capsule for selective recovery of Pd (II) from a binary metal solution. *J. Clean. Prod.* 288, 125648. <https://doi.org/10.1016/j.jclepro.2020.125648>.
- Yadav, N., Bisht, M., Nataraj, S., Venkatesu, P., Mondal, D., 2020. Multifunctional solvothermal carbon derived from alginate using ‘water-in-deep eutectic solvents’

- for enhancing enzyme activity. *Chem. Commun.* 56, 9659–9662. <https://doi.org/10.1039/D0CC03866K>.
- Yan, G., Viraraghavan, T., Chen, M., 2001. A new model for heavy metal removal in a biosorption column. *Adsorpt. Sci. Technol.* 19, 25–43. <https://doi.org/10.1260/0263617011493953>.
- Yang, B.-L., Goto, M., Goto, S., 1989. Affinity separation by the combined process of batch adsorption and fixed bed elution. *Colloid. Surface.* 37, 369–378. [https://doi.org/10.1016/0166-6622\(89\)80132-5](https://doi.org/10.1016/0166-6622(89)80132-5).
- Yang, J., Chen, Y., Gao, K., Li, Y., Wang, S., Xie, F., Jia, X., Song, H., 2021. Biomimetic superelastic sodium alginate-based sponges with porous sandwich-like architectures. *Carbohydr. Polym.* 272, 118527. <https://doi.org/10.1016/j.carbpol.2021.118527>.
- Zhang, R., Liang, B., Qu, T., Cao, B., Li, P., 2019a. High-performance sulfosuccinic acid cross-linked PVA composite pervaporation membrane for desalination. *Environ. Technol.* 40, 312–320. <https://doi.org/10.1080/09593330.2017.1388852>.
- Zhang, Z., Dong, Z., Wang, X., Dai, Y., Cao, X., Wang, Y., Hua, R., Feng, H., Chen, J., Liu, Y., Hu, B., Wang, X., 2019b. Synthesis of ultralight phosphorylated carbon aerogel for efficient removal of U(VI): batch and fixed-bed column studies. *Chem. Eng. J.* 370, 1376–1387. <https://doi.org/10.1016/j.cej.2019.04.012>.
- Zuhra, Z., Ali, S., Ali, S., Xu, H., Wu, R., Tang, Y., 2021. Exceptionally amino-quantitated 3D MOF@ CNT-sponge hybrid for efficient and selective recovery of Au (III) and Pd (II). *Chem. Eng. J.* 133367 <https://doi.org/10.1016/j.cej.2021.133367>.